ENGINEERING TRIPOS PART IB

Tuesday 1 June 1999 9.00 to 11.00

Paper 3

MATERIALS SOLUTIONS

1 *[Half marks available for brief outline of hetero and homogeneous nucleation. Graphs with limited supporting discussion (less detailed than that given) required for full marks].*
(a) Homogeneous nucleation involves the spontaneous formation of nuclei in the body of the solidifying liquid and therefore represents the idealised case. Heterogeneous nucleation is the formation of a solid phase on a surface which is determined by different energy balance criteria than homogeneous nucleation. An approximately spherical cap forms in heterogenoeus nucleation which effectively achieves the critical radius for growth with fewer atoms and hence decreases the degree of undercooling required. As a result heterogeneous nucleation is more common than homogeneous nucleation.

The extent to which a liquid transforms homogeneously to a solid depends on the thermodynamics and kinetics of the phase transformation (i.e. nucleation and growth). In general these are determined by the difference in the Gibbs free energy per unit volume, ΔG, between the phases, which is known as the driving force of the transformation. This subsequently determines the undercooling, $\Delta T = T_E - T$. The net total change in free energy ΔG_{tot} is given by ΔG ($=4/3\pi r^3 \Delta G$), which is a volume term and is negative, and the surface energy associated with creating new surface ($=4\pi r^2 \gamma$), which is an area term and is positive. $\Delta G_{tot}(r)$ therefore goes through a maximum with this maximum value $\Delta G_{tot}(r)^*$ representing the thermodynamic barrier to nucleation of the solid. The value of r at $\Delta G_{tot}(r)^*$ (i.e. r^*) corresponds to the critical size for phase growth. The nuclei will re-dissolve in the liquid if $r < r^*$.

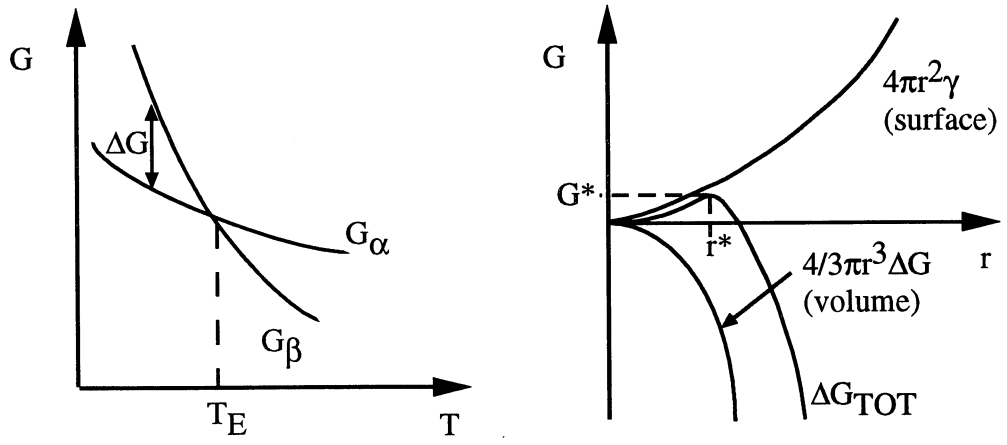

The overall grain nucleation rate depends both on the size of the thermodynamic barrier to be overcome and on the rate of diffusion of the molecules. At high temperature, therefore, the rate of grain nucleation is low since there is insufficient undercooling. At low temperatures the rate of grain nucleation is limited by a low diffusion rate {proportional to $\exp(-Q/RT)$}. Both effects are strongly temperature-dependent and act in opposition. As a result the rate of grain nucleation exhibits a maximum at a given temperature.

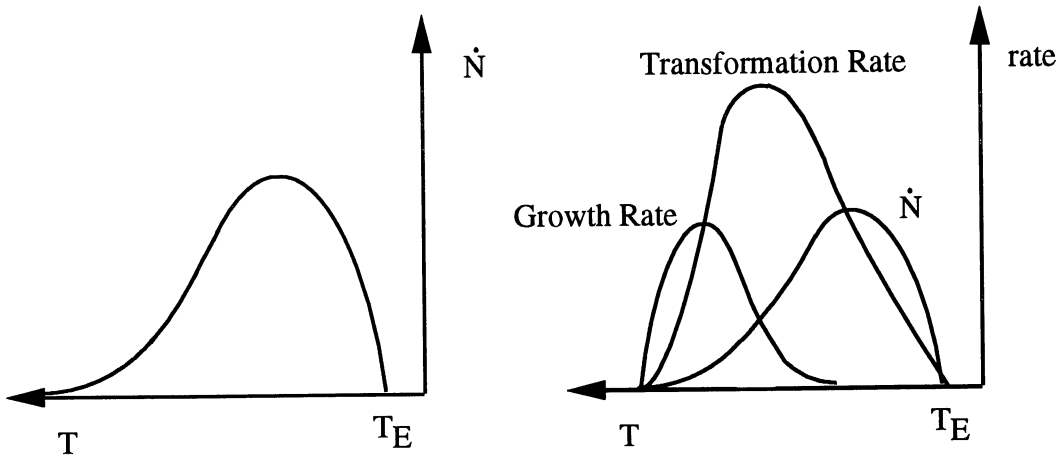

The growth rate of stable nuclei ($r > r^*$) depends on the driving force (proportional to ΔT) and the molecule diffusion rate. The overall transformation rate, therefore, is determined by the growth rate and the nucleation rate and is maximum for temperatures intermediate between those corresponding to maximum growth rate and maximum nucleation rate.

(b) $\Delta G_{tot} = \frac{4}{3}\pi r^3 \Delta G + 4\pi r^2 \gamma$ $\qquad \frac{\partial(\Delta G_{tot})}{\partial r} = 0$ as $r \rightarrow r^*$

i.e. $4\pi r^2 \Delta G + 8\pi r \gamma = 0$ $\qquad$ Hence $r^* = \frac{-2\gamma}{\Delta G}$

Also; $\Delta G = \frac{\Delta H}{T_E}(T_E - T)$ $\qquad$ Therefore $r^* = \frac{-2\gamma T_E}{\Delta H}\frac{1}{(T_E - T)}$ QED

(c) 175 molecules have a mass of $\frac{18.01 \times 175}{6.02 \times 10^{23}} = 5.24 \times 10^{-21}$g $= 5.24 \times 10^{-24}$kg.

$$\text{Volume} = \frac{\text{mass}}{\text{density}} = \frac{5.24 \times 10^{-24}}{0.92 \times 10^3} = 5.70 \times 10^{-27}\text{m}^3 = \frac{4}{3}\pi r^{*3}$$

$$r^* = \left(\frac{3 \times 5.70 \times 10^{-27}}{4\pi}\right)^{1/3} = 1.1\text{nm}$$

ΔH per unit volume = ΔH per unit mass $\times$ density $= -335 \times 10^3 \times 0.92 \times 10^3$
$= -3.08 \times 10^8$ Jm^{-3}.

$$T = T_E + \frac{2\gamma T_E}{\Delta H}\frac{1}{r^*} = 273 - \frac{2 \times 0.025 \times 273}{3.08 \times 10^8 \times 1.1 \times 10^{-9}} = 233\text{ K}$$

Undercooling for *homogeneous* nucleation ~ 40K.

Same volume required for heterogeneous nucleation.

$$\text{i.e.} \quad V = \frac{2\pi r^3}{3}\left(1 - \frac{3}{2}\cos\theta + \frac{1}{2}\cos^3\theta\right) = 5.70 \times 10^{-27}\text{m}^3$$

for $\theta = 10°$, $r^* = 19.9$nm. Hence T = 270.78K

Undercooling for *heterogeneous* nucleation ~ 2K.

Explains why ponds freeze first at surface/bank.

(d) 1. Casting (liquid-solid phase transformation); fine, high melting point, chemically compatible powders (inoculants) are added to melt to provide heterogeneous nucleation sites, leading to rapid nucleation. This produces a fine grain size, which is good for strength and toughness, and minimises segregation. 2. Solid-solid phase transformations; Ferrite phase nucleates on austenite grain boundaries to produce a fine grain size on cooling. 3. Seeded growth of silicon in single crystal fabrication. 4. Nucleation of growth at tip of turbine blade using controlled thermal gradient.

2 (a) Hardness; Ceramics are significantly harder than metals due to the large intrinsic lattice resistance to the motion of dislocations (σ_y ~ 5GPa c.f. ~200MPa for metals). Difference in lattice resistance to dislocation movement is due primarily to the nature of the primary bonds in metals in ceramics. Metallic bonds are non-directional and hence can be broken and re-formed along many lattice slip planes. Chemical bond in ceramics, however, are either ionic or covalent which do not have the directional properties of the metallic bond. Covalent bonds, for example, are directional and therefore difficult to break and re-form. Ionic bonds, on the other hand, are non-directional but only readily break and re-form along planes oriented at 45° to the major crystallographic axes due to the mutual repulsion of ions of common charge. As a result ceramics typically fracture before they yield.

Ductility; A large lattice resistance to dislocation movement in ceramics leads to brittleness and low fracture toughness, K_{IC}. Metals have a low lattice resistance and increased ductility. Ductility in metals is due to their ability to deform plastically at the crack tip. This involves dissipation of energy and subsequent relief of the build up in stress intensity. The higher lattice resistance in ceramics, on the other hand, makes slip difficult to achieve even when the stress is intensified at the crack tip. Energy, therefore, is generally not absorbed by the lattice at the crack tip and this builds up until brittle failure occurs.

Failure in ceramics is characterised statistically due to the wide distribution in flaw size. This distribution arises mainly due to manufacturing techniques (sintering, thermal cycling etc.) and determines critically the probability of survival of a given specimen.

(b) N specimens of SiC (25 in this case) of identical geometry with well-defined cross-section were tested to failure by the application of a tensile load. The specimens were then ranked, n, in order of strength from 1 (weakest) to N (strongest). The probability of failure (and hence survival) at each failure stress was calculated approximately as the fraction of the total number of specimens failing at stresses at this value or below. An alternative and more accurate method involves testing a batch of specimens at a stress σ_1

and calculating directly the fraction that survive. This is repeated for other batches at increasing test stress (σ_2, σ_3, etc.).

Weibull equation (Data Book); $$P_s(V) = \exp\left\{-\frac{V}{V_0}\left(\frac{\sigma}{\sigma_0}\right)^m\right\} \qquad (1)$$

For test specimens of identical volume;

$$\ln[P_s(V)] = -\left(\frac{\sigma}{\sigma_0}\right)^m \text{ and } \ln\left(\ln\left[\frac{1}{P_s(V)}\right]\right) = m\ln\left(\frac{\sigma}{\sigma_0}\right)$$

i.e. Weibull graph paper plots $\ln\left(\ln\left[\frac{1}{P_s(V)}\right]\right)$ and $\ln\left(\frac{\sigma}{\sigma_0}\right)$ on the ordinate and abscissa axes, respectively. Hence the construction of the axes.

When $\sigma = \sigma_0$, $P_s = 1/e = 0.37$. i.e. $\sigma_0(P_s = 37\%)$= **336 MPa**
[N.B. This is for a sample volume $V_0 = 0.5 \times 10^{-7}$ m^3]

From the graph;

σ (MPa)	P_s	$\ln\left(\ln\left[\frac{1}{P_s(V)}\right]\right)$	$\ln\left(\frac{\sigma}{\sigma_0}\right)$
238	0.95	-2.97	-0.345
358	0.10	0.834	0.063

$$\frac{\Delta \ln\left(\ln\left[\frac{1}{P_s(V)}\right]\right)}{\Delta \ln\left(\frac{\sigma}{\sigma_0}\right)} = m = \frac{-3.80}{-0.41} \approx \mathbf{9.31}$$

From the Weibull equation (1) with $P_s(V_1) = P_s(V_2) = 0.5$, $$\frac{\sigma(V_1)}{\sigma(V_2)} = \left(\frac{V_2}{V_1}\right)^{\frac{1}{m}}$$

Hence for a 5-fold increase in volume, $$\frac{\sigma(V_1)}{\sigma(V_2)} = 5^{1/9.31} \approx 1.189 \qquad (2)$$

Therefore; $\sigma(V_2) \approx \frac{\sigma(V_1)}{1.189}$ with $\sigma_{mean}(V_1) = 320$ MPa (i.e. $P_s = 50\%$)

$\sigma_{mean}(V_2)$ = **269 MPa**

(c) CSA = $(5 \times 10^{-3})^2 = 2.5 \times 10^{-5}$ m^2

$$V = (5 \times 10^{-3})^2 \times 10 \times 10^{-3} = 2.5 \times 10^{-7} \text{ m}^3 = 5V_0 \text{ in part (b)}$$

$$\sigma(V) = \frac{4000}{2.5 \times 10^{-5}} = 160 \text{ MPa}$$

Therefore, from (1) and (2) and using original values of σ_0 and V_0 in (b);

$$P_s(V) = \exp\left\{-\frac{5V_0}{V_0}\left(\frac{160}{336}\right)^{9.31}\right\} = \exp\left\{-5\left(\frac{160}{336}\right)^{9.31}\right\} = \mathbf{0.995}$$

(d) Stress in ligament = 2σ since cross-sectional area of notched region is twice that of unnotched region.

Survival probabilities are multiplicative; $P_s = P_s(V_1) \times 2\, P_s(V_2)$

Therefore; $P_s(V) = \exp\left\{-\left(\frac{1}{V_0\,\sigma_0^m}[(2\sigma)^m V_1 + \sigma^m(2V_2)]\right)\right\}$

The actual survival probability of the notched specimens is significantly less than that predicted by the above equation due to the concentration of stress at the corners of notches, which is not taken into account in the above calculation. Hence the assumption of uniform stress in the notched region is unreasonable.

The stress concentration factor K_t is given by $K_t \approx 2\left(\frac{a}{r_c}\right)^{1/2}$

where a is the notch depth and r_c is the radius of curvature at the corner of the notch (very small for 90° notches, < 0.1mm). K_t is therefore at least 10 at the notch corners, which is where the notched specimens will fail.

3 (a) *[Half marks available for the following general comments]* Plain carbon steels contain only residual concentrations of impurities other than carbon and a little manganese. Strength (yield and tensile) and hardness are determined by the microstructure of the steel. Cementite (Fe_3C) and martensite (α'- supersaturated BCC structure) act as a strengthening phases so higher C steels are generally stronger (increased Fe_3C). Cracks at the ferrite (α)/cementite interface, however, are easy to nucleate and hence ductility generally decreases with increasing C content. Properties, therefore, are a trade-off between strength (hardness) and toughness (ductility). The knee of the TTT diagram moves to longer times for increasing alloying (carbon content in this case) which increases its heat treatability.

Low carbon steels (< 0.25 wt% C): Microstructures usually consist of ferrite and pearlite. Martensite tends not to form given the low carbon content. Low carbon steels, therefore, are usually hardened by cold work or the generation of a fine grain microstructure (high undercooling), rather than by heat treatment. As a result low carbon steels tend to be relatively soft and weak but have generally high ductility and toughness. They are machinable, weldable and cheap. Applications include vehicle panels, nails, wire, pipes, sheet steel, structural members and pressure vessels.

Medium carbon steels (0.25 wt% < C < 0.6 wt%): Microstructure of tempered (rapidly cooled) α' consists of a fine dispersion of cementite particles in a continuous ferrite matrix. Slower cooling yields a ≈ 50/50 ferrite/pearlite microstructure. Martensite forms on quenching from austenite so medium carbon steels can be hardened by heat treatment. Most often used in tempered martensite condition which involves heating the steel to below the eutectoid temperature. Plain medium-carbon steels are the most hardenable but can only be heat treated successfully if martensite present in thin sections. Applications include crankshafts, bolts, tools (chisels, hammers, hacksaw blades) and knives.

High carbon steels (0.6 wt% < C < 1.4 wt%): Microstructure again consists of tempered α' but with a finer dispersion of cementite particles. Slower cooling yields a mixed microstructure of 100% pearlite and Fe_3C. High carbon steels form martensite on quenching from austenite and are almost always used in a hardened and tempered condition. These are the strongest, hardest and least ductile of the plain carbon steels and are particularly wear resistant. Generally more difficult than medium carbon steels to harden due to tendency of Fe_3C particles to coarsen. Applications include machine tools, die sets, springs and high-strength wire.

Use the lever rule to determine the proportion of Fe_3C in 1.5 wt. % carbon steel (measure lengths on phase diagram).

$$F_{Fe_3C} = \frac{C_{1.5} - C_\alpha}{C_{Fe_3C} - C_\alpha} = \frac{2}{8.7} \approx \mathbf{23\%}\ Fe_3C$$

(b) A: Austenite (phase)
B: Ferrite (phase)
C: Pearlite (microstructure)
D: Bainite (microstructure)
E: Martensite (phase)

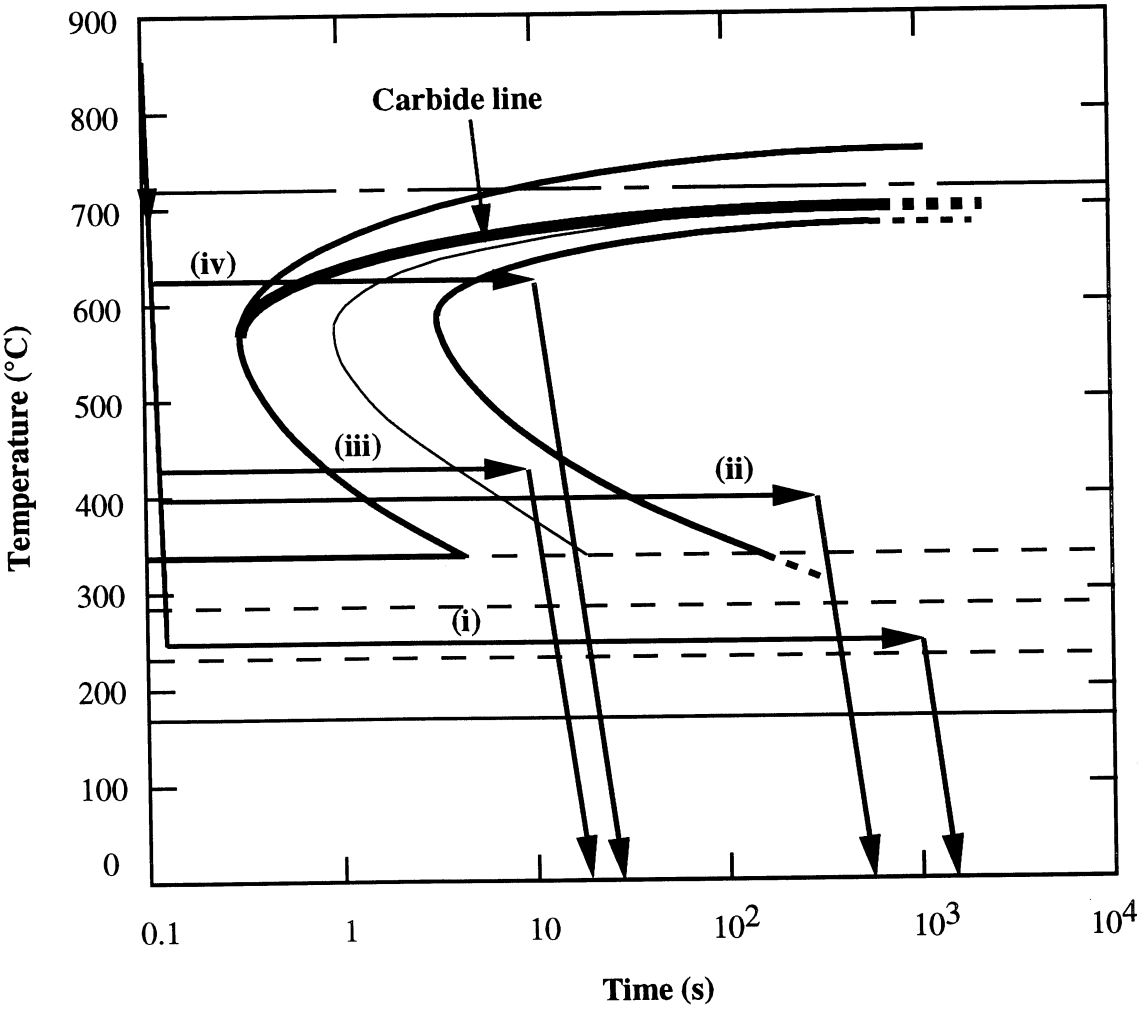

(i) Cool rapidly to 250 °C, hold for 1000 s; $\Rightarrow$ **100% martensite**

(ii) Cool rapidly to 400 °C, hold for 500 s; $\Rightarrow$ **100% bainite**

(iii) Cool rapidly to 450 °C, hold for 10 s; $\Rightarrow$ **75% bainite and 25% martensite**

(iv) Cool rapidly to 625 °C, hold for 10 s;
(proeutectoid) Ferrite forms initially until the carbide line is reached at which point fine pearlite forms (relatively low temperature). The approximate α/pearlite phase composition can be determined approximately by a lever rule type calculation between the 0%, carbide and 100% lines at 625 °C.

$\Rightarrow \approx$ **10% Ferrite (α) and 90% fine pearlite**

The critical cooling rate is the rate at which a steel should be cooled if it is to form only martensite (i.e. rate required to 'beat the nose' of the TTT curve). This is desirable if the mechanical properties of the steel are to be engineered by subsequent tempering. TTT diagrams are determined by quench-hold-quench sequences, however, and can therefore only be used reliably to predict the microstructures of steels produced by such a process.

(c) A new region in TTT diagram forms for steel with hypo-eutectoid composition (0.8 wt% C) in which ferrite forms from austenite at high temperature. The carbide line is the phase boundary between austenite+ferrite (A+B) and austenite+ferrite+pearlite (A+B+C) (i.e. the formation of ferrite terminates at the carbide line). Little ferrite forms towards the knee of the TTT diagram so pearlite contains < 0.8 wt% C for steel transformed in this region. Increasing ferrite phase content is produced above the carbide line at higher temperatures.

(d) The knee of the TTT diagram moves to shorter times for decreasing carbon content. This results in a higher critical cooling rate for the formation of undesired brittle phases (e.g. martensite) which enhances the weldability of low carbon steel.

4 (a) "Process model" is a mathematical description of the physical behaviour of a material during processing.

Process models allow:
(i) Cheap exploration of new operating regimes without interrupting production;
(ii) Re-design of equipment at low cost (e.g. dies for hot forming);
(iii) Greater understanding of origins of failure both during processing and later in service (e.g. cracking, distortion, porosity);

This results in:
(i) Improved productivity (lower scrap rates, greater processing speeds);
(ii) Prediction of microstructure and properties of final product (both average properties and variability);
(iii) Real time control.

(b)

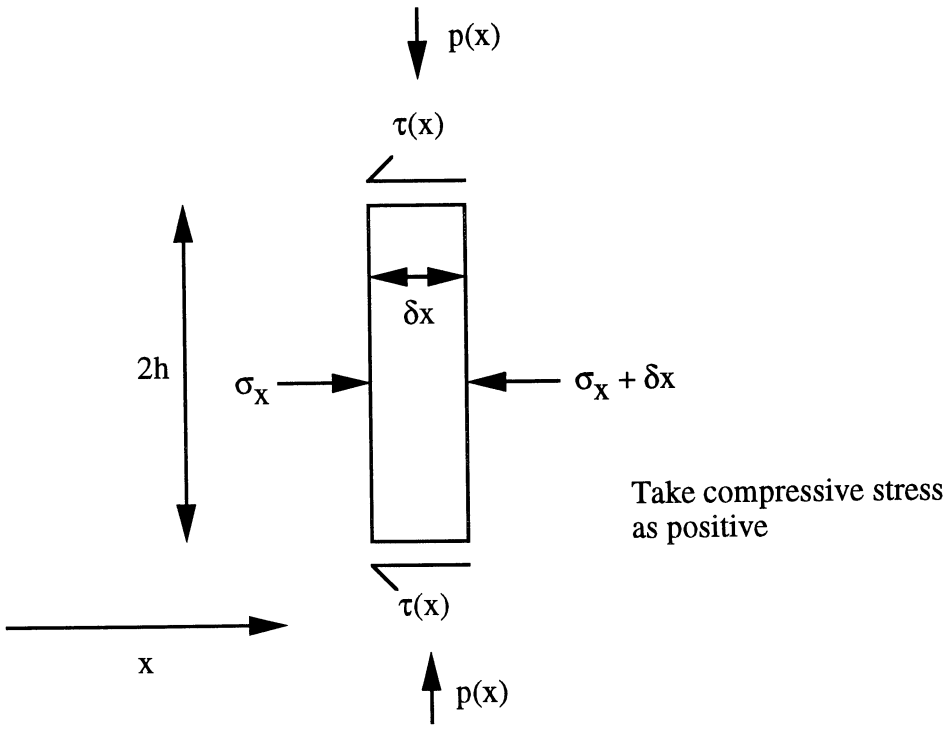

For $x > 0$ per unit length, the transverse compressive stress, σ_x, to the right is balanced by the transverse compressive stress, $\sigma_x+\delta\sigma_x$, and the frictional stress $2\tau(x)$ to the left;

$$(\sigma_x+\delta\sigma_x)\, 2h \times \ell - \sigma_x\, 2h \times \ell + 2\tau(x)\delta x \times \ell = 0$$

i.e. $$\frac{d\,\sigma_x}{d\,x} = -\frac{\tau(x)}{h} \qquad \text{(i)}$$

Assume Tresca yield criterion - τ small compared to p and σ_x so neglect (consider only principal stresses), i.e.; $p(x) - \sigma_x = \sigma_Y$

hence $$\frac{d\,p(x)}{d\,x} - \frac{d\,\sigma_x}{d\,x} = 0 \qquad \text{(ii)}$$

Therefore, from (i) and (ii) $$\mathbf{\frac{d\,p(x)}{d\,x} = -\frac{\tau(x)}{h}} \qquad \text{(iii)}$$

Substituting for $\tau(x) = \frac{m\sigma_Y}{2}$ in (iii); $$\frac{d\,p(x)}{d\,x} = -\frac{m\,\sigma_Y}{2h} \qquad \text{(iv)}$$

Boundary conditions: At edge of strip; $x = w$ and $\sigma_x = 0$ $\Rightarrow p = \sigma_Y$

Integrating (iv) with σ_Y as upper limit; $$\int_{p(x)}^{\sigma_Y} dp = -\int_x^w \frac{m\,\sigma_Y}{2h}\, dx$$

i.e. $p(x) = \sigma_Y \left[1 + \frac{m}{2}\left(\frac{w - x}{h}\right)\right]$ for $x > 0$.

Similarly, $p(x) = \sigma_Y \left[1 + \frac{m}{2}\left(\frac{w + x}{h}\right)\right]$ for $x < 0$

p(x) vs. x across the entire width of the bar is known as the "friction hill";.

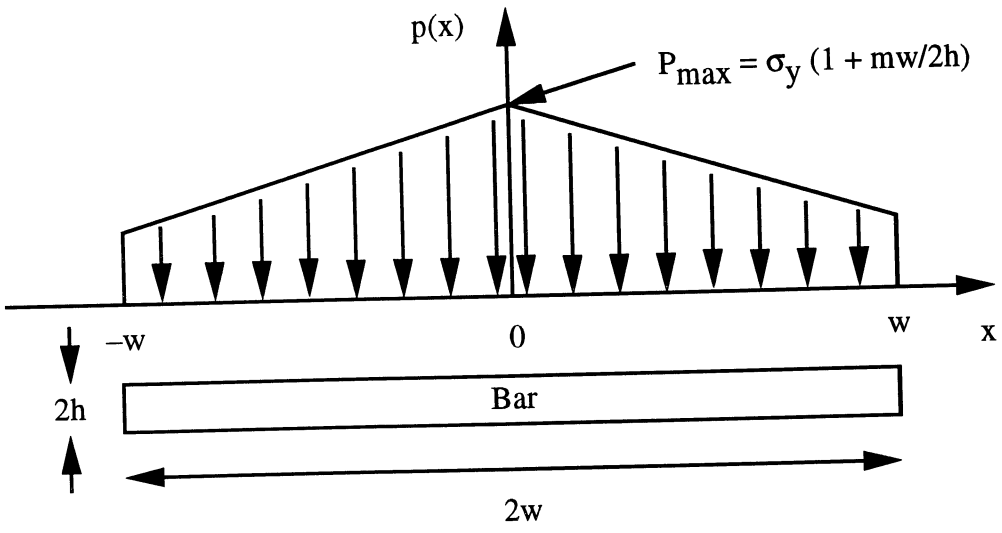

(c) σ_Y = 40MPa for aluminium alloy at forging temperature.

$p_{max} = \sigma_Y \left(1 + \frac{m\,w}{2\,h}\right) = 40 \times 10^6 \times \left(\frac{0.8 \times 1.5}{1}\right) = 88$ MPa at centre of bar.

$p_{min} = \sigma_Y = 40$ MPa at edge of bar. Hence $\bar{p} = \frac{88 + 40}{2} \times 10^6 =$ **64 MPa**

$F = 64 \times 10^6 \times 0.2 \times 0.03 = 3.84 \times 10^5$ N = **384 kN**.

(d) The analysis is most relevant to the forging of aluminium at elevated temperature (i.e. hot forging). This reduces work hardening in the bar (dynamic recovery and recrystallisation), hence the yield stress can be assumed to be constant. Also friction is high in hot forging since difficult to lubricate.

5 (a) Objective and constraint equations for shear strength performance index;

Objective in each case is to minimise mass: $m = \pi R^2 L \rho$ (i)

L = length, ρ = density of cylinder

Constraint is that τ must not exceed shear yield strength τ_y; $\tau_y = \frac{2T}{\pi R^3}$ (ii)

Rearrange (ii) and eliminate free variable (R) in (i);

$$R = \left(\frac{2\,T}{\pi\,\tau_y} \right)^{\frac{1}{3}} \qquad m = (\,2\sqrt{\pi}\;T\,L^{3/2}\,)^{2/3} \times \frac{\rho}{\tau_y^{2/3}}$$

Also; $\tau_y = \frac{\sigma_y}{2}$ i.e. $m = (\,4\sqrt{\pi}\;T\,L^{3/2}\,)^{2/3} \times \frac{\rho}{\sigma_y^{2/3}}$

Hence *maximise* M1 for minimum mass $M1 = \frac{\sigma_y^{2/3}}{\rho}$ (iii)

(b) Taking logs of both sides of equation (iii) and rearranging;

$$\log \sigma_y = 3/2 \log \rho + 3/2 \log M1$$

Hence equivalent materials lie on straight line of gradient 3/2 on materials selection chart.

Tensile yield strength of quenched and tempered low alloy steel = 1560 MPa, ρ = 7800 kgm^{-3}. Plot this point on chart and put straight line of slope 3/2 through it. Region required lies above 300 MPa and above this line (see chart).

(c) From part (a); $T = \frac{\tau_{max}\,\pi\,R^3}{2}$

From Structures Data Book; $\tau_{max} = G\gamma$ and $\gamma = \frac{\phi\,R}{L}$

Objective and constraint equations for torsional stiffness performance index;

Constraint is torsional stiffness T/ϕ;

Hence $T = G\,\pi\,R^4\,\frac{\phi}{2\,L} \quad \Rightarrow \quad \frac{T}{\phi} = \frac{G\,\pi\,R^4}{2\,L}$ (iv)

Objective again is to minimise mass: $m = \pi\,R^2\,L\,\rho$ (i)

Eliminate free variable (R); $m = \left(\frac{2\,T}{\phi}\,\pi\,L^3 \right)^{1/2} \times \frac{\rho}{\sqrt{G}}$

Hence *maximise* M2 for minimum mass $M2 = \frac{G^{1/2}}{\rho}$

ENGINEERING TRIPOS PART IB PAPER 3 MATERIALS

Materials Selection Chart for Question 5

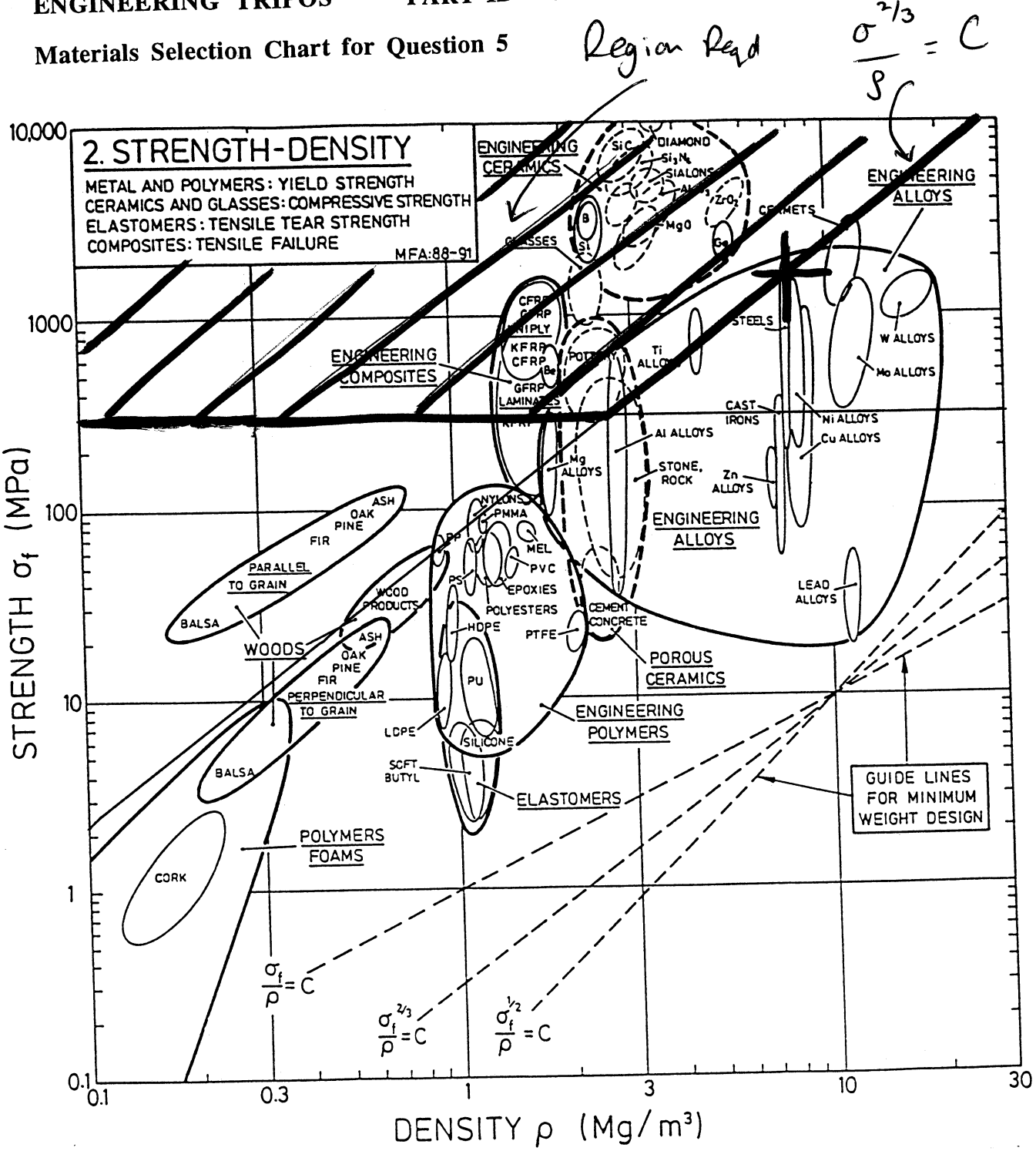

Fig. 6. This figure should be annotated and handed in as part of your solution to question 5.

Material	Density, ρ (kg m^{-3})	σ_f (MPa)	G (≈3/8E) (GPa)	M1 × 10^3	M2 × 10^3
Titanium Alloy	4500	960	43.1	21.6	1.46
GFRP	1800	200	11.3	19.0	**1.87**
Aluminium Alloy	2800	600	26.3	**25.4**	1.83
Low Alloy Steel	7800	780	78.8	10.9	1.14

Material	Strength ranking	Stiffness ranking
Titanium Alloy	2	3
GFRP	3	1
Aluminium Alloy	1	2
Low Alloy Steel	4	4

Need to calculate actual mass of drive shaft for each material. Hence require L and T to evaluate m for maximum strength and L, T and ϕ to evaluate m for maximum stiffness.

(d) Need to consider other factors which limit the choice of each material for manufacture of the drive shaft compared with alloy steel. i.e.;

(i) Titanium alloy: Mainly cost and low stiffness per unit mass.

(ii) GFRP: Cost, toughness (determines whether the shaft will fail under impact), formability (GFRP tubes are easy to make but are difficult to join), manufacturability (GFRP difficult to shape).

(iii) Aluminium alloy: Low tensile strength (< 300 MPa for some alloys)

6 (a) There are 5 general strength-limiting processes of thermoplastics. In order of increasing temperatures, these are;

1. Brittle fracture ($T < 0.75\ T_g$)
Fast fracture criterion when inherent flaw size reaches the critical crack size, a_0 (typically a few microns). PMMA fails by this process.

2. Cold drawing ($T_g - 50°C$)
Long chain polymer molecules are drawn out which leads to orientation effects along the draw direction. This process is analogous to work hardening in metals. Stress becomes amplified at a flaw and neck forms and propagates. Polyethylene, polycarbonate and nylon fail by this process.

3. Crazing ($T_g - 100°C$)
Some thermoplastics with higher T_g craze under tension before they cold draw. Each craze is a microcrack abridged by highly-oriented molecular chains which resist its propagation. Crazes typically form at the tip of pre-existing cracks. PMMA and polystyrene fail by this process.

4. Shear banding (T_g – 100°C)
Thermoplastics which craze under tension may deform plastically under tension by shear banding. A shear band forms by the local accumulation of strain which leads to the formation of a multiplicity of intersecting bands. These increase in number and grow in width. PMMA and polystyrene fail by this process.

5. Viscous flow ($T > T_g$)
Viscous flow is the time-dependent strain which occurs in a thermoplastic following the application of a load. The long chain polymer molecules slide over each other in the process, which is usually non-recoverable. Polymers under low applied load fail eventually by this process. Silicone polymer ('silly putty') is a particularly common example.

(b) Strain rate of dashpot ; $\dot{\varepsilon}_{dashpot} = \frac{\sigma(t)}{\eta}$, strain rate of spring; $\dot{\varepsilon}_{spring} = \frac{\dot{\sigma}(t)}{E}$

i.e. $\dot{\varepsilon}_{total} = \dot{\varepsilon}_{dashpot} + \dot{\varepsilon}_{spring} = \frac{\sigma(t)}{\eta} + \frac{\dot{\sigma}(t)}{E}$

But $\dot{\varepsilon} = 0$ for $t > 0$ (constant strain), hence $\frac{\sigma(t)}{\eta} + \frac{1}{E}\frac{d\,\sigma(t)}{dt} = 0$

with solution; $\sigma(t) = \sigma(0) \exp\left[-\frac{t}{t_0}\right]$

Differentiate and substitute back into equation; $\frac{\sigma(0)\, e^{-t/t_0}}{\eta} - \frac{\sigma(0)\, e^{-t/t_0}}{E\, t_0} = 0$

i.e. $t_0 = \frac{\eta}{E}$

Thermoplastics relax, or creep, following the application of a tensile load (*time-dependent strain*) which results in alleviation of applied stress, as described by the equation. This process dominates for all stress in the visco-elastic regime, i.e. above the glass transition temperature, and is therefore most dominant at high temperature. Elastic behaviour dominates at low stress and temperatures where polymers fail typically by brittle fracture.

(c) $\sigma(0) = \frac{150}{(3 \times 10^{-3})^2 \times \pi} = \mathbf{5.3\ MPa}$ $\varepsilon(0) = \frac{2.6}{100}$ $E = \frac{100 \times 5.1 \times 10^6}{2.6} = \mathbf{0.2\ GPa}$

From relaxation test; $\sigma(t) = \sigma(0) \exp\left[-\frac{t}{t_0}\right]$ $t_0 = \frac{-t}{\ln\left[\frac{\sigma(t)}{\sigma(0)}\right]}$ $= \frac{-t}{\ln\left[\frac{F(t)}{F(0)}\right]}$

$t_0 = \frac{-10}{\ln\left[\frac{28}{150}\right]} = \mathbf{6s}$ [Check; $t_0 = \frac{\eta}{E}$, $\eta = 1.2$ GPa s $E = \frac{\eta}{t_0} = \frac{1.2 \times 10^9}{6} = 0.2$ GPa]

The polymer can be identified from its tensile modulus (page 9 of the Materials Data Book). Hence the subject of the test is **LDPE**.

(d) This model is entirely phenomenological and cannot be used to describe the physical process responsible for the deformation of the polymer. Hence it is of no use in describing the microscopic behaviour of the material.